Showcasing research from Professor Guo-Xin Jin's laboratory, Department of Chemistry, Fudan University, Shanghai, China.

s-Block metal ions induce structural transformations between figure-eight and double trefoil knots

The Chinese knot is a very iconic Chinese handicraft, which reflects the wisdom and culture of China. The Chinese knot has several beautiful meanings including unity, association, affinity and being forever concentric. Our research on molecular knots is reflective of the structure and artistic beauty of the Chinese. Here, we describe the reversible topological transformation between figure-eight and double trefoil knots, which was induced by introducing and removing K^+ ions with 18-crown-6 based on the coordination reaction between K^+ ions and amide groups.

As featured in:

See Guo-Xin Jin *et al.*, *Chem. Sci.*, 2020, **11**, 1226.

ROYAL SOCIETY
OF **CHEMISTRY**

rsc.li/chemical-science

Chemical Science

EDGE ARTICLE

Check for updates

s-Block metal ions induce structural transformations between figure-eight and double trefoil knots†‡

Li-Long Dang, Xiang Gao, Yue-Jian Lin and Guo-Xin Jin 🔟 *

The formation of two types of heterobimetallic molecular knots, double trefoil and trefoil knots, induced by s-block metal ions, is presented. Coordination of K⁺, Ca²⁺, Sr²⁺ or Ba²⁺ ions with amide groups plays a crucial role in the formation of these trefoil knots. Remarkably, the reversible topological transformation between a figure-eight knot and double trefoil or trefoil knots can be induced by coordination of s-block metal ions to amide groups. X-ray crystallographic data and NMR experiments support the structural assignments.

Introduction

Molecular knots, a nontrivial form of chemical topology, are ubiquitously found in proteins[1,2] and DNA[3] and have attracted increasing attention of chemists owing to their fascinating aesthetics and the biomimetic properties of synthetic molecular knots.[4–11] A variety of small-molecule knots with different crossings have now been synthesised, either by designed methods or serendipitous discovery.[12–28] Recent reports of the synthesis of 8_{19},[29] $+3_1 \# +3_1 \# +3_1$ composite knots[11] and granny knots[30] have marked considerable progress in the synthesis of molecular knots. Moreover, a range of structural transformations of molecular knots to other topologically interesting compounds, such as solomon links or monocyclic ring, have also been observed recently.[5,9] However, there are very few reports of transformations from one type of molecular knot to another.[31] Thus, the adjustment of the spatial arrangements of ligands in order to achieve a reversible transformation between two types of molecular knot remains a formidable challenge.

Figure-eight knot, as its name implies, will take on the shape of "8" through the connections of building blocks utilizing coordination and/or covalent bonds, ultimately forming a closed loop, which has four alternating crossings in the reduced representation. Thus, it is also called 4_1 knot. We recently reported that both figure-eight (4_1) and trefoil knot species[32] could be prepared by treating amide and ester

derivatives with [Cp*M]-based (M = Ir, Rh) connecting units under identical reaction conditions. By comparing these knot topologies, we hypothesised that the presence or absence of intramolecular hydrogen bond interactions likely determines the different outcomes of the reactions (Fig. 1).[33] Thus, if the C=O or N–H groups of the amide sites could be shielded, the formation of intramolecular hydrogen bonds would be hampered, which might result in other knot topologies.

Pioneering work in this area has proven that amide oxygen atoms are good coordination sites, and a series of interlocked [2]-, [3]catenanes and molecular knots have been formed depending on the coordination between amide groups and metal ions.[34,35] A typical example is the fact that three 2,6-pyridinedicarboxamide ligands entwining a lanthanide(III) ion provide a molecular trefoil knot by ring-closing olefin metathesis.[36] Thus, this behaviour of amide oxygen atoms coordinated to metal ions may be used to change the self-assembly mechanism of figure-eight knot by fixing the spatial arrangement of an amide ligand **L** with secondary metal ions in the synthesis of trefoil knot. Intriguingly, when the secondary metal ions are removed, the system could potentially transform into a molecular figure-eight knot.
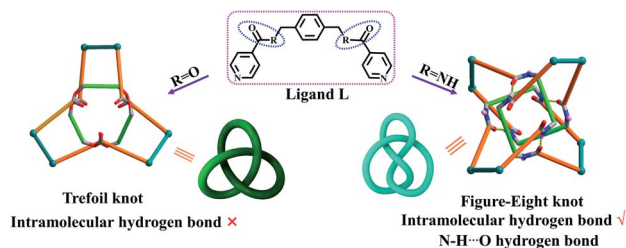
Shanghai Key Laboratory of Molecular Catalysis and Innovative Materials, State Key Laboratory of Molecular Engineering of Polymers, Department of Chemistry, Fudan University, Shanghai 200438, P. R. China. E-mail: gxjin@fudan.edu.cn

† Dedicated to Professor Ekkehardt Hahn on the occasion of his 65th birthday.

‡ Electronic supplementary information (ESI) available: CCDC 1965232 (**1**), 1964477 (**2**), 1965067 (**3a**), 1964537 (**3b**) and 1964536 (**4**). For ESI and crystallographic data in CIF or other electronic format see DOI: 10.1039/c9sc05796j

Fig. 1 Schematic representation of stick models and topological images of a figure-eight knot and trefoil knot obtained using amide and ester ligands.[32]

Herein, we present the synthesis of two types of molecular knots, double trefoil and trefoil knots, obtained by introducing secondary metal ions (K^+, Ca^{2+}, Sr^{2+} or Ba^{2+} ions) into the self-assembly process of amide ligand **L** with Cp*Rh edge unit **E** (**L** + **E** = figure-eight knot). X-ray crystallographic data show that the central K^+ ion bridges trefoil tangles of opposite handedness by coordination with six amide oxygen atoms, leading to the realisation of a novel double trefoil knot **1**. In contrast, alkaline earth metal cations induce the formation of a series of trefoil knots due to the coordination with three amide groups, and small molecules or OTf^- ions. Of particular note is that all the amide oxygen atoms of trefoil knot **4** were found to be coordinated to two Ba^{2+} cations, which results in an octanuclear configuration (Fig. 2). In addition, the ^{1}H NMR spectra demonstrate that the addition of secondary metal ions into a solution of figure-eight knot in CD_3OD induces the formation of heterometallic trefoil knots. However, removal of K^+, Ca^{2+}, Sr^{2+} and Ba^{2+} ions from these knots by adding 18-crown-6 promoted transformations to figure-eight knot.

Results and discussion

Self-assembly of a double-trefoil knot (1) based on complete coordination of K^+ ions with amide groups

Our initial hypothesis was that the coordination of K^+ ions with amide sites could take place in a self-assembly process, thereby hindering the generation of intramolecular N–H⋯O hydrogen bonds and finally resulting in new reaction products. We carried out an experiment involving the addition of K^+ ions prior to self-assembly: the yellow solid **1** (yield: 86.4%) was obtained by treating **E** with ligand **L** and 2.0 equiv. of KNO_3 in methanol after 6 h of stirring under ambient conditions. The structure of **1** was confirmed by NMR spectroscopy, electrospray ionization mass spectrometry (ESI-MS), and single-crystal X-ray diffraction analysis.

NMR spectroscopic experiments were carried out to explore the behaviour of **1** in CD_3OD. The simpler ^{1}H NMR spectrum obtained (relative to that expected for figure-eight knot) clearly supported the formation of a new topological structure (Fig. S7, ESI‡). The ^{1}H NMR signals show two doublets at δ 8.60, 7.14 ppm and one singlet at δ 1.73 ppm for the protons of pyridinyl and Cp* groups, and the protons of two 2,2′-bisbenzimidazole (**BiBzlm**) appear as two sets of multiplets at δ 8.15–8.12 and 7.70–7.48 ppm. However, the signals of the phenyl groups show large upfield shifts to 1.0–4.5 ppm, which might be due to the tight π–π stacking of phenyl groups (Fig. S8, ESI‡).[30] The ^{1}H DOSY NMR spectrum of **1** shows that the aromatic and Cp* signals are associated with a single diffusion constant ($D = 2.6 \times 10^{-10}$ m^{-2} s^{-1}), suggesting that only one stoichiometry of assembly is formed (Fig. S10, ESI‡).

Single crystals of **1** were obtained by slow diffusion of diethyl ether vapor into a solution of **1** in methanol. Its solid-state structure indicated that complex **1** contains twelve Cp*Rh vertexes and two potassium ions, denoted $K1^+$ and $K2^+$ in Fig. 2. The two potassium ions are in different positions in the framework and play specific roles in the formation of **1**. The

Fig. 2 Synthesis of double trefoil knot **1**, trefoil knots **2**, **3** and **4**; structural transformation between figure-eight knot and **1**, **2**, **3**, **4** can be observed by introduction and/or removal of K^+, Ca^{2+}, Sr^{2+}, Ba^{2+} ions.

central K1$^+$ ion acts as a bridge to connect two trefoil tangles ($+3_1$ and -3_1) by coordination with six amide oxygen atoms, forming a double trefoil knot. The K2$^+$ ion is bound to another three amide oxygen atoms from the $+3_1$ or -3_1 trefoil tangle, with one OTf$^-$ anion and two CH$_3$OH molecules. However, there exist three possible connection forms between two trefoil knots in solution ($+3_1$ connecting with $+3_1$; -3_1 connecting with -3_1; $+3_1$ connecting with -3_1). In the solid state, $+3_1$ and -3_1 trefoil knots being connected can be caused by appropriate stacking of **1** (Fig. 3). Furthermore, ESI-MS data of **1** in methanol showed peaks at m/z 2680.66 assigned to $[\mathbf{1} - 2\text{CH}_3\text{OH} - 3\text{OTf}^-]^{3+}$, further confirming the structure of **1** as a double trefoil knot and indicating that complex **1** exhibits remarkable stability in solution (Fig. S31, ESI‡). The formation of double trefoil knot **1** verifies that intramolecular N–H···O hydrogen bond interactions play a crucial role in the stabilisation of figure-eight knot. The coordination of the K$^+$ ions with the amide groups is likely the main reason for the synthesis of structure **1** by virtue of hindering the formation of intramolecular N–H···O hydrogen bonds. This result provides a new concept for the construction of increasingly complex topological structures and studying the conversion between amide-containing supramolecular compounds.

We next sought to investigate whether NO$_3^-$ anions have an influence on the formation of double trefoil knot **1**. Thereby a self-assembly experiment by using KOTf instead of KNO$_3$ was carried out under the same reaction conditions. Structure **1** was again obtained, thereby demonstrating that NO$_3^-$ anions had no significant effect on the formation of the complex **1**.

The double trefoil knot **1** includes two K$^+$ ions in different chemical environments. However, the ^{1}H NMR spectrum shows the same signal pattern as that of a trefoil knot, most likely due to that the weak coordination interactions between K$^+$ ion and C=O groups.[37,38]

We continued our investigation of the ability of K$^+$ ions to destroy intramolecular N–H···O hydrogen bonds by attempting the K$^+$-mediated structural unlinking of figure-eight knot (Fig. 2) to the double trefoil knot **1**. Thus, ^{1}H NMR spectroscopic experiments were carried out to explore the behaviour of K$^+$ ions in a methanol solution of figure-eight knot. Upon addition of a slight excess of KNO$_3$ into a CD$_3$OD solution of figure-eight

knot in 1.5 mM, a new set of signals appeared that was consistent with the signals of compound **1**. However, the conversion was very low and reached only 26.1% after 24 h stirring under ambient conditions. This demonstrates that once the N–H···O hydrogen bonds of figure-eight knot are formed, destroying them and forming a double trefoil knot is difficult (Fig. 4).

As outlined above, we speculated that the coordination between K$^+$ ions and amide sites hinders the formation of intramolecular N–H···O hydrogen bonds in the self-assembly process resulting in the double trefoil knot **1**. However, this conjecture might be invalidated if the trefoil monomers of **1** can exist as a stable entity when the K$^+$ ions are removed. In an attempt to obtain trefoil monomers without K$^+$ ions, we sought to remove the K$^+$ ions of the double trefoil knot by using the known K$^+$ scavenger 18-crown-6.[39,40] However, attempts to remove the K$^+$ ions by adding 18-crown-6 to a CD$_3$OD solution of **1** while maintaining the trefoil monomer topology proved unsuccessful. We observed that the ^{1}H NMR signals of complex **1** decreased, while those of complex figure-eight knot increased over time, when a slight excess of 18-crown-6 was added to a previously prepared solution of **1** in CD$_3$OD (4.0 mM with respect to Cp*Rh), indicating a gradual structural unraveling of **1** to figure-eight knot (Fig. 5). The conversion reached 86.2% after 24 h of reaction time. This result further proves that in the absence of secondary K$^+$ ions, figure-eight knot has a higher stability than the trefoil knot structure in methanol solution. Furthermore, density functional theory (DFT) calculation also supports this result.[41] (Fig. S34 and S35, ESI‡).

Self-assembly of trefoil knots 2, 3, and 4 based on partial coordination of Ca^{2+}, Sr^{2+} and Ba^{2+} cations with amide groups

The high charge density, large ionic radii and higher coordination numbers (6–10) of alkaline earth metal ions Ca^{2+}, Sr^{2+} and Ba^{2+} has led to their use in the construction of metal–organic frameworks with good thermal stability.[42–48] In order to explore the effects of Ca^{2+}, Sr^{2+} and Ba^{2+} cations on the self-
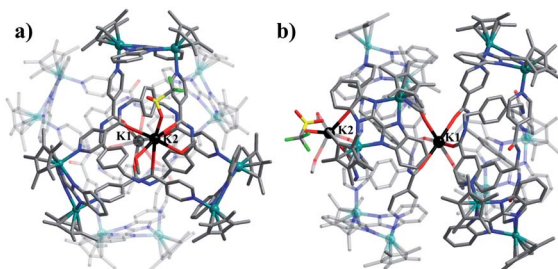

Fig. 3 Single-crystal X-ray structure of double trefoil knot **1**. Top view (a) and side view (b). Counteranions and hydrogen atoms are omitted for clarity. All hydrogen atoms, anions, and solvent molecules are omitted for clarity except for coordination anions of potassium ions. Rh teal; K gray; N blue; C gray.
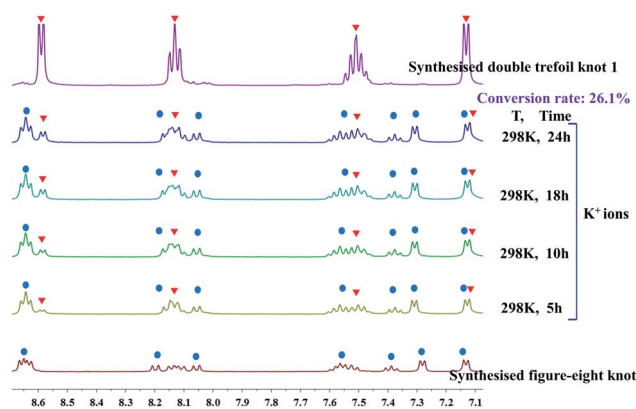

Fig. 4 Partial ^{1}H NMR spectra (CD$_3$OD, 400 MHz, 298 K) concerning structural unlinking transformation of figure-eight knot to double trefoil knot **1** induced by K$^+$ ions. Blue circles denote signals of figure-eight knot; red triangles denote double signals of the trefoil knots.
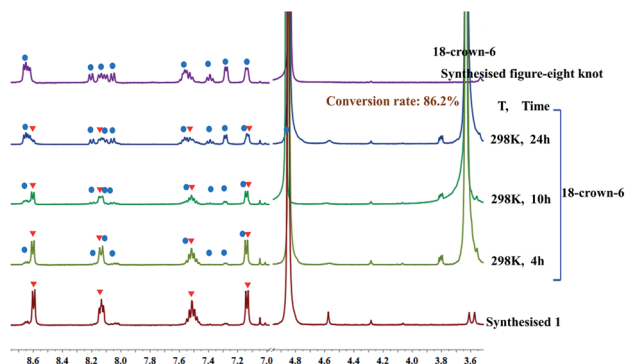
Fig. 5 Partial ^{1}H NMR spectra (CD$_3$OD, 400 MHz, 298 K) showing the structural unlinking transformation of double trefoil knot **1** to figure-eight knot by removing K$^+$ ions with 18-crown-6. Red triangles denote signals of the double trefoil knot, blue circles denote signals of the figure-eight knot.

assembly of **E** and **L** in a methanol solution, identical reactions of **E** and **L** were performed under ambient conditions with addition of Ca(NO$_3$)$_2$·4H$_2$O, Sr(NO$_3$)$_2$ or Ba(NO$_3$)$_2$ instead of KNO$_3$. Accordingly, complexes **2**, **3** and **4** were obtained in yields of 87.3%, 82.3% and 84.0%. The structures of **2**, **3** and **4** were confirmed by NMR spectroscopy, electrospray ionization mass spectrometry (ESI-MS), and single-crystal X-ray diffraction analysis.

The ^{1}H NMR spectrum of **2** in CD$_3$OD exhibits one sharp singlet at $\delta = 1.73$ ppm corresponding to a single Cp*Rh environment, in marked contrast to the spectrum of figure-eight knot, suggesting a new topology (Fig. S13, ESI‡). The ^{1}H DOSY NMR spectrum of **2** showed that the aromatic and Cp* proton signals were associated with a single diffusion constant, suggesting that only one stoichiometry of assembly was formed (Fig. S15, ESI‡).

Assembly **2** was crystallised by diffusion of diethyl ether into its methanol solution and its trefoil knot structure was elucidated by single-crystal X-ray crystallography. Similarly to figure-eight knot, the unit **E** and amide ligand **L** combine with assistance from π–π and CH–π interactions. The single Ca^{2+} cation was found to be bound to three **L** amide oxygen atoms and three OTf$^-$ ions in a κ^6 fashion. The environment around the Ca^{2+} cation is best described as slightly distorted octahedral. The Ca–O$_{amide}$ (2.2956(6)–2.2956(11) Å) and Ca–O$_{OTf}$ (2.3323(6)–2.3323(11) Å) distances are comparable to those found in previous work.[49] In addition, the remaining three amide groups form stable N–H···O intermolecular hydrogen bond interactions with a OTf$^-$ anion (2.92 Å) (Fig. 6a and b). ESI-MS data also indicated that the prominent peaks at $m/z = 2048.23$ ([**2** − 2OTf$^-$]$^{2+}$) is in good agreement with their theoretical distribution (Fig. S32, ESI‡), suggesting that the structure remains intact in solution.

The Sr^{2+} cation is slightly larger than the Ca^{2+} cation, thus we speculated that Sr^{2+} could similarly coordinate with amide oxygen atoms and hinder the formation of intramolecular N–H···O hydrogen bonds, ultimately inducing formation of a new topological structure. The ^{1}H NMR and ^{1}H DOSY NMR

Fig. 6 Single-crystal X-ray structures of **2** and **3a**. Top view (a) and side view (b) of complex **2**; Top view (c) and side view (d) of complex **3a**. Counteranions and hydrogen atoms are omitted for clarity. All hydrogen atoms, anions, and solvent molecules are omitted for clarity except for coordination anions of calcium and strontium cations. Rh teal; Ca violet; Sr green; N blue; C gray; O red; S yellow; F bright green.

($D = 2.7 \times 10^{-10}$ m^{-2} s^{-1}) spectra of **3** were recorded in CD$_3$OD. As expected, the ^{1}H NMR spectra of **3** show clear differences with those of figure-eight knot (Fig. S19, ESI‡). The ^{1}H DOSY NMR showed a single diffusion coefficient ($D = 2.7 \times 10^{-10}$ m^{-2} s^{-1}), suggesting a single structure in solution (Fig. S21, ESI‡). Single crystals were obtained by slow diffusion of diethyl ether into a methanol solution and the solid-state structure of **3** was determined to also be a trefoil knot by X-ray diffraction analysis. In addition, two isomers, **3a** and **3b**, are present in the solid state.

The single-crystal X-ray diffraction analysis of **3a** and **3b** reveals that both are topological enantiomers with the same $P6_3$ point group, with either positive or negative crossings in the unit cells of **3a** or **3b**, respectively, in the solid state (Fig. 7), consistent with reported structures.[50] The Sr^{2+} cation is
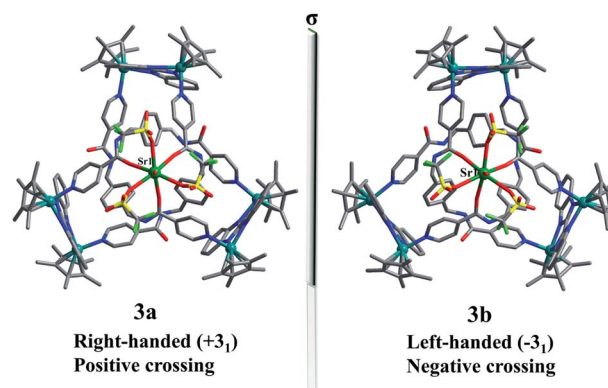

Fig. 7 Skeleton representation of the right-handed trefoil knot ($+3_1$) of **3a** (left); skeleton representation of the left-handed trefoil knot (-3_1) of **3b** (right).

coordinated in a κ^7 fashion with a single-capped octahedron geometry. The metal ion is coordinated to three amide oxygen atoms, three triflate anions, and one H_2O molecule. In addition, another triflate anion forms N–H$\cdots$O intermolecular hydrogen bonds with the remaining three amide groups. The coordination of Ca^{2+} or Sr^{2+} cations with amide groups thus effectively hinders the formation of intramolecular N–H$\cdots$O hydrogen bonds and leads to the generation of trefoil knots. Additionally, ESI-MS data of **3** in methanol shows a peak at m/z 2072.21 assigned to ([$3 - H_2O - 2OTf^-$]$^{2+}$), which further confirms the structure of **3** as a trefoil knot and indicates that complex **3** exhibits remarkable stability in solution (Fig. S33, ESI‡).

A closer look at the trefoil topologies induced by K^+, Ca^{2+} and Sr^{2+} ions showed that some amide groups are not involved in the coordination, which form intermolecular N–H$\cdots$O hydrogen bonds with a OTf$^-$ ion. We hypothesised that a more strongly-binding metal ion may achieve complete coordination of the six amide groups of a single trefoil knot. The Ba^{2+} cation was selected to test this hypothesis.[51] As expected, the octanuclear trefoil knot **4** was formed by the introduction of Ba(NO$_3$)$_2$, in which the six amide groups coordinate to two Ba^{2+} cations.

The ^{1}H NMR spectrum of **4** in CD$_3$OD showed all of the expected signals corresponding to the protons of a trefoil knot (Fig. S25, ESI‡), and a single diffusion coefficient ($D = 2.4 \times 10^{-10}$ m^{-2} s^{-1}) was observed in a ^{1}H DOSY NMR experiment (Fig. S27, ESI‡). These observations clearly demonstrate that trefoil knot **4** is the unique species in solution.

Single crystals of complex **4** suitable for XRD analysis were obtained by diffusion of diethyl ether into a saturated solution of **4** in methanol. Complex **4** crystallises in space group $C2/c$ with the topology of a 3_1 knot according to the Alexander–Briggs notation. The observation of 1 : 1 ratio of both enantiomers ($\Lambda\Lambda\Lambda$ and $\Delta\Delta\Delta$) is consistent with reported structure (Fig. S6, ESI‡).[52] Close-contact analysis of the structure reveals a trefoil knot arrangement similar to a distorted trigonal bipyramidal configuration composed of two types of metal ion (Rh^{III} and Ba^{II}) and two types of organic ligand (**L** and **BiBzlm**). The structure is held together by both edge-to-face-type CH–π interactions (3.39 Å) and parallel-displaced π–π interactions (of

interlayer distance 3.72 Å) between phenyl moieties and two nearby pyridyl moieties of three **L** ligands (Fig. 8). This is in marked contrast to figure-eight knot, in which intramolecular N–H$\cdots$O hydrogen bond interactions play a crucial role in the stabilisation of the topological structure. The barium cations (Ba1^{2+} and Ba2^{2+}) of trefoil knot **4** are both octacoordinate. Similar to the Ca^{2+}/Sr^{2+} cations of **2/3**, the Ba1^{2+} and Ba2^{2+} cations each bind to three amide oxygen atoms. However, the remaining coordination sites of the two barium cations are occupied by different units. Ba1^{2+} is bound to CH$_3$OH, DMSO and H$_2$O molecules, and one OTf$^-$ ion in an O,O'-chelating form. Meanwhile, Ba2^{2+} is bound to three CH$_3$OH molecules, one H$_2$O and one OTf$^-$ ion. Again, the interaction of the Ba^{2+} cations and the amide groups hinders the formation of intramolecular N–H$\cdots$O hydrogen bond interactions and thereby alters the reaction direction.

Structural transformations between figure-eight knot and trefoil knots induced by Ca^{2+}, Sr^{2+} and Ba^{2+} cations

Trefoil knots being induced by Ca^{2+}, Sr^{2+} and Ba^{2+} cations encourages us to explore the effects of these cations on the transformation of figure-eight to trefoil knots in methanol solution. Compared to K^+ cation, Ca^{2+} cation, due to higher valence state and smaller ionic radius, may have greater binding energy and result in higher transformation efficiency of figure-eight to trefoil knots. In addition, previous work[53,54] has reported that the binding energies of metal–oxygen increase with decreasing metal ions size ($Ba^{2+} < Sr^{2+} < Ca^{2+}$ ions). Thus, transformation efficiency of figure-eight to trefoil knots may also increase (TE(Ba^{2+}) < TE(Sr^{2+}) < TE(Ca^{2+})) as the cation radius decreases (r(Ba^{2+}) > r(Sr^{2+}) > r(Ca^{2+}) ions). Three ^{1}H NMR monitoring experiments were performed in methanol solution over a period of 24 h. We observed the slow transformations of figure-eight knot to trefoil knots upon respective addition of calcium, strontium or barium salts to CD$_3$OD solutions of figure-eight knot. After 24 h, the conversion to the corresponding trefoil knot species was 44.7% for Ca^{2+}, 40.1% for Sr^{2+} and 27.2% for Ba^{2+} (Fig. S17, S23 and S29, ESI‡). The experimental data are consistent with the expected reactivity based on ionic radii for these alkali earth metal cations, which also indicate that Ca^{2+}, Sr^{2+}, Ba^{2+} cations have greater capacity to destroy the intramolecular N–H$\cdots$O hydrogen bonds of figure-eight knot to induce their unravelling and formation of trefoil knots than K^+ ions (transformation efficiency: 26.1%) (Fig. 9).
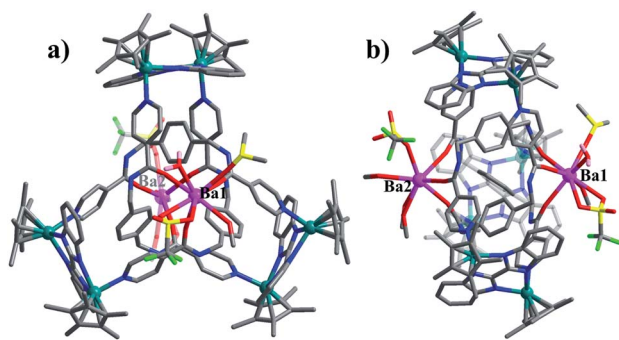

Fig. 8 Molecular structure of trefoil knot **4**. Top view (a) and side view (b). Counteranions and hydrogen atoms are omitted for clarity. All hydrogen atoms, anions, and solvent molecules are omitted for clarity except for coordination solvent molecules or anions. Rh teal; Ba pink; N blue; C gray; O red; S yellow; F bright green.

Fig. 9 The topological transformation between figure-eight and trefoil knots by adding and removing Ca^{2+} or Sr^{2+} ions.

The heavier alkaline-earth cations Ca^{2+}, Sr^{2+} and Ba^{2+} are also known to form stable complexes with 18-crown-6.[55] Thus, addition of 18-crown-6 to trefoil knots **2**, **3** and **4** resulted in their structural unlinking and formation of figure-eight knot. NMR spectroscopic data clearly show the gradual transformation of the trefoil knots to figure-eight knot upon addition of a slight excess of 18-crown-6 to CD_3OD solutions of complexes **2–4** (Fig. S18, S24 and S30, ESI‡). After 24 h, all of these transformations had reached conversions above 85.0% by NMR spectroscopy, further indicating that Ca^{2+}, Sr^{2+} and Ba^{2+} cations play a critical role in the formation and stabilisation of the respective heterometallic trefoil knots.

Conclusions

In conclusion, s-block metal cations can induce structural transformations between figure-eight knot and double or single trefoil knots by adding or removing K^+, Ca^{2+}, Sr^{2+} or Ba^{2+} ions. These double or single trefoil knots can also be obtained by employing the corresponding metal salts in the self-assembly process (**E** + **L**). Interestingly, in the case of K^+, these ions bridge two trefoil monomers of opposite handedness, resulting in the synthesis of a double trefoil knot. In contrast, Ca^{2+}, Sr^{2+} or Ba^{2+} cations facilitate the construction of single trefoil knots. Additionally, 18-crown-6 can trigger topological unlinking of double and single trefoil knots to figure-eight knot by removing the s-block metal ions. The destruction and formation of N–H⋯O intramolecular hydrogen bonds is determined to be the main cause of the observed structural transformations between these molecular knots. We believe that a deeper understanding of the topological transformations in amide-containing assemblies induced by the presence or absence of s-block metal ions will be helpful in the future construction of bespoke architectures and responsive supramolecular systems, opening up new vistas in the field of functional molecules and materials.

Conflicts of interest

There are no conflicts to declare.

Acknowledgements

Notes and references

1 L. F. Liu, R. E. Depew and J. C. Wang, *J. Mol. Biol.*, 1976, **106**, 439–452.

2 F. Ziegler, N. C. H. Lim, S. S. Mandal, B. Pelz, W. P. Ng, M. Schlierf, S. E. Jackson and M. Rief, *Proc. Natl. Acad. Sci. U. S. A.*, 2016, **113**, 7533–7538.

3 J. S. Richardson, *Nature*, 1977, **268**, 495–500.

4 J. E. Beves, B. A. Blight, C. J. Campbell, D. A. Leigh and R. T. McBurney, *Angew. Chem., Int. Ed.*, 2011, **50**, 9260–9327.

5 S. D. P. Fielden, D. A. Leigh and S. L. Woltering, *Angew. Chem., Int. Ed.*, 2017, **56**, 11166–11194.

6 H. N. Zhang, W. X. Gao, Y. J. Lin and G. X. Jin, *J. Am. Chem. Soc.*, 2019, **141**, 16057–16063.

7 O. Safarowsky, M. Nieger, R. Fröhlich and F. Vögtle, *Angew. Chem., Int. Ed.*, 2000, **39**, 1616–1618.

8 J. F. Ayme, G. Gil-Ramírez, D. A. Leigh, J. F. Lemonnier, A. Markevicius, C. A. Muryn and G. Zhang, *J. Am. Chem. Soc.*, 2014, **136**, 13142–13145.

9 B. B. Guo, Y. J. Lin and G. X. Jin, *Chem.–Eur. J.*, 2019, **25**, 9721–9727.

10 V. Marcos, A. J. Stephens, J. Jaramillo-Garcia, A. L. Nussbaumer, S. L. Woltering, A. Valero, J. F. Lemonnier, I. J. Vitorica-Yrezabal and D. A. Leigh, *Science*, 2016, **352**, 1555–1559.

11 L. Zhang, A. J. Stephens, A. L. Nussbaumer, J. F. Lemonnier, P. Jurček, I. J. Vitorica-Yrezabal and D. A. Leigh, *Nat. Chem.*, 2018, **10**, 1083–1088.

12 T. Prakasam, *et al.*, *Angew. Chem., Int. Ed.*, 2013, **52**, 9956–9960.

13 R. S. Forgan, J.-P. Sauvage and J. F. Stoddart, *Chem. Rev.*, 2011, **111**, 5434–5464.

14 J. Guo, P. C. Mayers, G. A. Breault and C. A. Hunter, *Nat. Chem.*, 2010, **2**, 218–222.

15 N. Ponnuswamy, F. B. L. Cougnon, J. M. Clough, G. D. Panto□ and J. K. M. Sanders, *Science*, 2012, **338**, 783–785.

16 M. Feigel, R. Ladberg, S. Engels, R. Herbst-Irmer and R. Fröhlich, *Angew. Chem., Int. Ed.*, 2006, **45**, 5698–5702.

17 J. F. Ayme, J. E. Beves, D. A. Leigh, R. T. McBurney, K. Rissanen and D. Schultz, *Nat. Chem.*, 2012, **4**, 15–20.

18 L. Zhang, A. J. Stephens, J. F. Lemonnier, L. Pirvu, I. J. Vitorica-Yrezabal, C. J. Robinson and D. A. Leigh, *J. Am. Chem. Soc.*, 2019, **141**, 3952–3958.

19 V. Marcos, A. J. Stephens, J. Jaramillo-Garcia, A. L. Nussbaumer, S. L. Woltering, A. Valero, J. F. Lemonnier, I. J. Vitorica-Yrezabal and D. A. Leigh, *Science*, 2016, **352**, 1555–1559.

20 C. O. Dietrich-Buchecker and J.-P. Sauvage, *Angew. Chem., Int. Ed.*, 1989, **28**, 189–192.

21 D. H. Busch, *J. Inclusion Phenom. Mol. Recognit. Chem.*, 1992, **12**, 389–395.

22 P. E. Barran, H. L. Cole, S. M. Goldup, D. A. Leigh, P. R. McGonigal, M. D. Symes, J. Wu and M. Zengerle, *Angew. Chem., Int. Ed.*, 2011, **50**, 12280–12284.

23 D. H. Busch, *Science*, 1971, **171**, 241–248.

24 J. F. Ayme, J. E. Beves, C. J. Campbell and D. A. Leigh, *Chem. Soc. Rev.*, 2013, **42**, 1700–1712.

25 C. Lincheneau, B. Jean-Denis and T. Gunnlaugsson, *Chem. Commun.*, 2014, **50**, 2857–2860.

26 D. M. Engelhard, S. Freye, K. Grohe, M. John and G. H. Clever, *Angew. Chem., Int. Ed.*, 2012, **51**, 4747–4750.

27 J.-P. Sauvage, *Angew. Chem., Int. Ed.*, 2017, **56**, 11080–11093.

28 Y. Segawa, M. Kuwayama, Y. Hijikata, M. Fushimi, T. Nishihara, J. Pirillo, J. Shirasaki, N. Kubota and K. Itami, *Science*, 2019, **365**, 272–276.

29 J. J. Danon, A. Krüger, D. A. Leigh, J. F. Lemonnier, A. J. Stephens, I. J. Vitorica-Yrezabal and S. L. Woltering, *Science*, 2017, **355**, 159–162.

30 J. J. Danon, D. A. Leigh, S. Pisano, A. Valero and I. J. Vitorica-Yrezabal, *Angew. Chem., Int. Ed.*, 2018, **130**, 14029–14033.

31 N. Ponnuswamy, F. B. L. Cougnon, G. D. Pantoș and J. K. M. Sanders, *J. Am. Chem. Soc.*, 2014, **136**, 8243–8251.

32 L. L. Dang, Z. B. Sun, W. L. Shan, Y. J. Lin, Z. H. Li and G. X. Jin, *Nat. Commun.*, 2019, **10**, 2057.

33 E. A. Neal and S. M. Goldup, *Chem. Commun.*, 2014, **50**, 5128–5142.

34 F. Zapata, O. A. Blackburn, M. J. Langton, S. Faulkner and P. D. Beer, *Chem. Commun.*, 2013, **49**, 8157–8159.

35 M. J. Langton, O. A. Blackburn, T. Lang, S. Faulkner and P. D. Beer, *Angew. Chem., Int. Ed.*, 2014, **53**, 11463–11466.

36 G. Zhang, G. Gil-Ramírez, A. Markevicius, C. Browne, I. J. Vitorica-Yrezabal and D. A. Leigh, *J. Am. Chem. Soc.*, 2015, **137**, 10437–10442.

37 Y. Inokuchi, T. Ebata, T. R. Rizzo and O. V. Boyarkin, *J. Am. Chem. Soc.*, 2014, **136**, 1815–1824.

38 K. Tsubaki, D. Tanima, Y. Kuroda, K. Fuji and T. Kawabata, *Org. Lett.*, 2006, **8**, 5797–5800.

39 T. Dudev and C. Lim, *J. Am. Chem. Soc.*, 2009, **131**, 8092–8101.

40 A. Torvisco and K. Ruhlandt-Senge, *Inorg. Chem.*, 2011, **50**, 12223–12240.

41 L. L. Gong, D. T. Zhang, C. Y. Lin, L. P. Zhang and Z. H. Xia, *Adv. Energy Mater.*, 2019, **9**, 1902625–1902633.

42 D. Banerjee and J. B. Parise, *Cryst. Growth Des.*, 2011, **11**, 4704–4720.

43 S. L. Cai, S. R. Zheng, Z. Z. Wen, J. Fan and W. G. Zhang, *Cryst. Growth Des.*, 2012, **12**, 3575–3582.

44 M. L. Foo, S. Horike and S. Kitagawa, *Inorg. Chem.*, 2011, **50**, 11853–11855.

45 J. A. Dolyniuk, H. He, A. S. Ivanov, A. I. Boldyrev, A. Bobev and K. Kovnir, *Inorg. Chem.*, 2015, **54**, 8608–8616.

46 X. G. Yang, L. F. Ma and D. P. Yan, *Chem. Sci.*, 2019, **10**, 4567–4572.

47 Z. Gao, Z. W. Yu, F. Q. Liu, X. F. Feng and F. Luo, *Inorg. Chem.*, 2019, **58**, 11500–11507.

48 X. G. Yang, X. M. Lu, Z. M. Zhai, Y. Zhao, X. Y. Liu, L. F. Ma and S. Q. Zang, *Chem. Commun.*, 2019, **55**, 11099–11102.

49 Y. Sarazin, B. Liu, T. Roisnel, L. Maron and J. F. Carpentier, *J. Am. Chem. Soc.*, 2011, **133**, 9069–9087.

50 K. E. Horner, M. A. Miller, J. W. Steed and P. M. Sutcliffe, *Chem. Soc. Rev.*, 2016, **45**, 6432–6448.

51 D. W. Fu, Y. Zhang, H. L. Cai, H. M. Zhu, X. Y. Chen and R. G. Xiong, *J. Mater. Chem.*, 2012, **22**, 17525–17530.

52 L. Zhang, D. P. August, J. K. Zhong, G. F. S. Whitehead, I. J. Vitorica-Yrezabal and D. A. Leigh, *J. Am. Chem. Soc.*, 2018, **140**, 4982–4985.

53 S. E. Rodriguez-Cruz, R. A. Jockusch and E. R. Williams, *J. Am. Chem. Soc.*, 1999, **121**, 1986–1987.

54 E. D. Glendening and D. Feller, *J. Phys. Chem.*, 1996, **100**, 4790–4797.

55 Y. Tatematsu, S. Kato, N. Nakata, M. Ebihara, O. Niyomura, K. Sugamata, M. Yukimoto and M. Minoura, *Dalton Trans.*, 2018, **47**, 9787–9794.